Bureau of Engineering Research
The University of Texas at Austin
Austin, Texas

CAR 91-2

TEST AND ANALYSIS PROCEDURES FOR UPDATING MATH MODELS OF SPACE SHUTTLE PAYLOADS

by

Roy R. Craig, Jr.

NASA Contract No. NAG 9-346
May, 1991

TEST AND ANALYSIS PROCEDURES FOR UPDATING MATH MODELS OF SPACE SHUTTLE PAYLOADS

Roy R. Craig, Jr.*

Final Report

NASA Grant NAG 9-346
Lyndon B. Johnson Space Center
Houston, TX

Report No. CAR 91-2

Center for Aeromechanics Research
Department of Aerospace Engineering and Engineering Mechanics
Bureau of Engineering Research
College of Engineering
The University of Texas at Austin
Austin, Texas 78712

May, 1991

*John J. McKetta Energy Professor of Engineering, Department of Aerospace Engineering and Engineering Mechanics

ACKNOWLEDGEMENTS

The research that is summarized in this report was supported by Grant NAG 9-346 from the NASA Johnson Space Center. The interest of Mr. David Hamilton, the Technical Officer for the grant, is greatly acknowledged. The research described in this report was conducted primarily by Mr. Chee-Yun Li and Mr. Hsin-Hsen Huang.

ABSTRACT

Over the next decade or more, the Space Shuttle will continue to be the primary transportation system for delivering payloads to Earth orbit. Although a number of payloads have already been successfully carried by the Space Shuttle in the payload bay of the Orbiter vehicle, there continues to be a need for evaluation of the procedures used for verifying and updating the math models of the payloads.

The verified payload math model is combined with an Orbiter math model for the coupled-loads analysis, which is required before any payload can fly. Several test procedures have been employed for obtaining data for use in verifying payload math models and for carrying out the updating of the payload math models.

Research under the present grant and a follow-on NASA grant, NAG 9-484, has been directed at the evaluation of test/update procedures for use in the verification of Space Shuttle payload math models. This report summarizes three research tasks: a study of free-interface test procedures[1], a literature survey and evaluation of model update procedures[2], and the design and construction of a laboratory "payload simulator"[3].

TABLE OF CONTENTS

List of Figures

Chapter 1

INTRODUCTION

Over the next decade or more the Space Shuttle will continue to be the primary transportation system for delivering payloads to Earth orbit. Among the payloads will be various Space Station modules. Although a number of payloads have been successfully carried by the Space Shuttle in the payload bay of the Orbiter vehicle, there is a pressing need for evaluation of the procedures for verifying and updating the math models of the payloads. Several test procedures have been employed for obtaining data for use in verifying payload math models: a free-free modal test, a free-free modal test of the payload with mass-loaded interfaces[4], a free-free modal test including computation of residuals[5, 6], a fixed-interface modal test[7], a fixed-interface modal test supplemented by a modal test of the support structure[8], and an impedance test[9].

References [4] through [9] discuss some of the advantages and limitations of the various test methods and indicate that there is no general concensus on the "best" way to acquire data for use in math model updating. The newest and least well-known test procedure is the so-called "impedance" procedure employed by Blair and Vadlamudi on the Hubble Space Telescope[9]. The theoretical basis for this free-interface test method is explored at some depth in Ref.[1].

The payload math model must be combined with the Orbiter math model for the coupled-loads analysis, which is required before any payload can fly. The most frequently employed format for the payload math model is the Craig-Bampton model[10], developed by the Principal Investigator[11]. The payload math model may also be supplied in the form of mass and stiffness matrices. To provide background for the study of combined test/update procedures and their application to Space Shuttle payloads, an in-depth survey of literature on the topic of math model updating was conducted. Mathematical descriptions of several methods used to determine the locations of model errors (error localization methods), and mathematical descriptions of several methods used to update the analytical math models using experimental data are provided in Ref.[2].

Finally, to provide a test-bed for evaluating various modal test / model update procedures giving special emphasis to component interface behavior, a "payload simulator" structure was designed and fabricated. The design of the simulator, and preliminary modal tests are described in Ref.[3].

The remainder of this report is devoted to brief summaries of Refs.[1] through [3].

Chapter 2

SYSTEM IDENTIFICATION AND MODEL UPDATING FOR STRUCTURAL COMPONENTS (REF.1)

A popular analytical model for representing the dynamics of structural components, such as Space Shuttle payloads, is the Craig-Bampton model[10, 11]. This model is based on representation of the dynamics of the component in terms of fixed-interface normal modes and constraint modes. Frequently, a fixed-interface (fixed-base) modal test is employed to validate the model.* Due to the difficulties inherent in fixed-base modal testing (cost, flexibility of the "fixed" base, etc.) alternatives in the form of free-suspension modal testing are investigated in Ref.[1]. A brief description of the Craig-Bampton modeling procedure is given first. This is followed by an analysis of frequency response functions in Craig-Bampton coordinates. Examples are provided for both undamped and damped lumped-parameter systems and also for undamped continuous systems (rods and beams).

*This test does not directly verify the accuracy of the constraint mode terms in the model.

2.1 The Structure Model

Before any dynamical analysis can be performed on a structure, a mathematical representation of the said structure must be created. There are basically two categories of analytical models, namely, continuous models and discrete-parameter models. A continuous model has an infinite number of degrees-of-freedom (DOF), and it describes the physical motion of the original structure exactly. However, this kind of model is governed by a set of partial differential equations, which may be difficult to work with both analytically and computationally.

On the other hand, discrete-parameter models are governed by ordinary differential equations, which can be solved relatively easily. A discrete model may be constructed by either the lumped-mass approach or the assumed-modes approach (which includes the finite element method). In lumped-mass models, the mass of the system is assumed to be concentrated in a small number of point masses, or in rigid bodies, while springs and dampers are assumed to be massless. In the assumed-modes approach, a discrete model may be generated by assuming motion of the form

$$u(x,t) = \sum_{i=1}^{N} \phi_i(x)\eta_i(t) \tag{2.1}$$

where $\phi_i(x)$ is an admissible function and N is the number of degrees-of-freedom to be specified by the analyst. The equations of motion for the resulting N-DOF model are then derived using Lagrange's equations[12]. This is the basis of the finite element method.

2.2 Component Modes

At times, a large structure may be treated as a group of components connected together and then analyzed by a powerful method called the component mode synthesis (CMS) method[13]. An example of such a system may be represented by Fig. 2.1. The physical coordinates of each component (α or β) may be divided into the boundary coordinates, b, and the interior coordinates, i. The attractiveness of the component mode synthesis method lies in its ability to preserve the essential dynamical characteristics of the component while reducing the original set of coordinates considerably. Through a Ritz transformation, the physical coordinates for the component may be expressed in terms of a reduced set of modal coordinates.

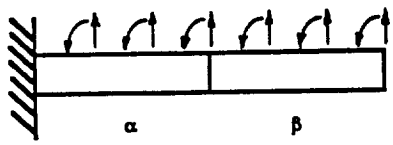

Figure 2.1: A two-component cantilever beam model.

The three most commonly used modes, or Ritz vectors, to describe a component are: normal modes, constraint modes, and attachment modes. These, again, are made up of a wide variety of modes such as the fixed-interface, free-interface and loaded-interface normal modes, and so on. Due to the scope of

this report, only fixed-interface normal modes and constraint modes will be discussed. Interested readers are referred to Reference[13] for further details.

Fixed-interface normal modes are generated by solving an eigenvalue problem of the following form while keeping all the interface coordinates fixed.

$$[k_{ii}][\Phi_{ii}] - [m_{ii}][\Phi_{ii}][\Lambda_{ii}] = [0] \tag{2.2}$$

where $[k_{ii}]$ is an i × i stiffness matrix, $[m_{ii}]$ is an i × i mass matrix, $[\Phi_{ii}]$ is the i × i "normal mode matrix," $[\Lambda_{ii}]$ is the i × i diagonal eigenvalue matrix, and i is the number of interior degrees-of-freedom.

For a 2-component cantilever beam, two fixed-interface normal modes are illustrated in Fig. 2.2. One of the useful properties of the normal modes

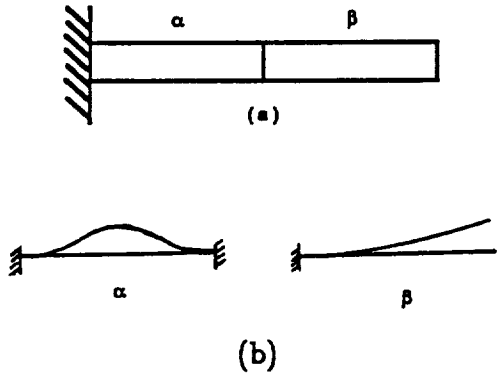

Figure 2.2: Fixed-interface normal modes. (a) A two-component cantilever beam. (b)A normal mode for each component.

is that when they are normalized with respect to the mass matrix $[m_{ii}]$, the following orthogonality relationships hold.

$$[\Phi_{ii}]^T[m_{ii}][\Phi_{ii}] = [I_{ii}] \quad , \quad [\Phi_{ii}]^T[k_{ii}][\Phi_{ii}] = [\Lambda_{ii}] = diag(\lambda_i) \tag{2.3}$$

where $[\Phi_{ii}]$ is the i $\times$ i "normal mode matrix" described in Eq. (2.2). Now, the full normal mode matrix is given by

$$[\Phi_i] = \begin{bmatrix} [0_{bi}] \\ [\Phi_{ii}] \end{bmatrix} \tag{2.4}$$

A constraint mode is generated, on the other hand, by applying a unit displacement to one of the boundary coordinates statically while holding the rest of the boundary coordinates fixed. The set of constraint modes may be defined as[13]

$$\begin{bmatrix} [k_{bb}] & [k_{bi}] \\ [k_{ib}] & [k_{ii}] \end{bmatrix} \begin{bmatrix} [I_{bb}] \\ [\Phi_{ib}] \end{bmatrix} = \begin{bmatrix} [R_{bb}] \\ [0_{ib}] \end{bmatrix} \tag{2.5}$$

where $[R_{bb}]$ is the set of reaction forces at the boundary coordinates. From the lower row-partition of Eq. (2.5)

$$[\Phi_{ib}] = -[k_{ii}]^{-1}[k_{ib}] \tag{2.6}$$

The constraint mode matrix is thus given by

$$[\Phi_b] = \begin{bmatrix} [I_{bb}] \\ [\Phi_{ib}] \end{bmatrix} = \begin{bmatrix} [I_{bb}] \\ -\ [k_{ii}]^{-1}\ [k_{ib}] \end{bmatrix} \tag{2.7}$$

Another useful property of the two kinds of modes, defined by Eqs.(2.2) and (2.7), is that they are orthogonal with respect to the stiffness matrix, that is,

$$\begin{aligned} [\Phi_i]^T [k] [\Phi_b] &= [0_{ib}] \\ [\Phi_b]^T [k] [\Phi_i] &= [0_{bi}] \end{aligned} \tag{2.8}$$

Several constraint modes are illustrated in Fig. 2.3.

2.3 Frequency Response of an Undamped System in Craig-Bampton Coordinates

Once a model is generated, the next step is to derive an appropriate equation of motion to describe the physical behavior of the model. For linear

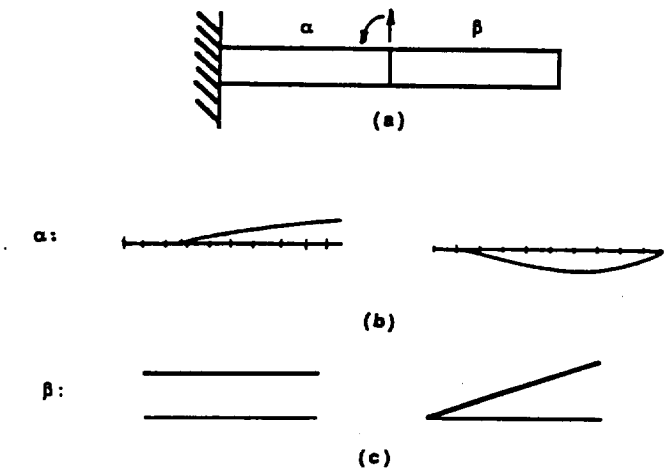

Figure 2.3: Constraint modes. (a) A two-component cantilever beam. (b) Constraint modes for component α. (c) Constraint modes for component β.

finite DOF structural systems, the equation of motion takes the following form

$$[m]\ddot{\vec{u}}(t) + [c]\dot{\vec{u}}(t) + [k]\vec{u}(t) = \vec{f}(t) \tag{2.9}$$

where $[m]$ is a n $\times$ n mass matrix, $[c]$ is a n $\times$ n damping matrix, $[k]$ is a n $\times$ n stiffness matrix, $\vec{u}$ is a displacement vector of order n, $\vec{f}$ is a force vector of order n, and n is the total number of degrees-of-freedom of the system.

The component mode synthesis method discussed briefly in preceding sub-section consists of a wide variety of methods, but the most straightforward and accurate method is the so-called Craig-Bampton method[11]. This method is specified, for example, in Ref. 10 as one to be used by Space Shuttle payload contractors. With this method, the component coordinates are separated into the interior coordinates and the boundary coordinates. The interior coordinates

are then related to a set of fixed-interface normal modes, while the boundary coordinates are related to a set of constraint modes. This special combination of modes is also sometimes referred to as "Craig-Bampton coordinates."

For an undamped system, the equation of motion reduces to

$$[m]\ddot{\vec{u}}(t) + [k]\vec{u}(t) = \vec{f}(t) \tag{2.10}$$

The physical coordinates, $\vec{u}$, may be represented in terms of modal coordinates, $\vec{\eta}$, by the following coordinate transformation

$$\vec{u}(t) = [\Phi]\vec{\eta}(t) = \begin{bmatrix} [\Phi_b] & [\Phi_i] \end{bmatrix} \begin{bmatrix} \vec{\eta}_b(t) \\ \vec{\eta}_i(t) \end{bmatrix} \tag{2.11}$$

where $[\Phi]$ is the component mode matrix consisting of the constraint mode matrix, $[\Phi_b]$, and the fixed-interface normal mode matrix, $[\Phi_i]$.

By substituting Eq. (2.11) into Eq. (2.10), we get

$$[m][\Phi]\ddot{\vec{\eta}}(t) + [k][\Phi]\vec{\eta}(t) = \vec{f}(t)$$

Premultiplying the above equation by $[\Phi]^T$ and using the properties of Eqs. (2.3) and (2.8), the equation of motion for an undamped vibrating system becomes

$$([\Phi]^T[m][\Phi])\ddot{\vec{\eta}}(t) + ([\Phi]^T[k][\Phi])\vec{\eta}(t) = [\Phi]^T\vec{f}(t)$$

or

$$\begin{bmatrix} [\Phi_b]^T[m][\Phi_b] & [\Phi_b]^T[m][\Phi_i] \\ [\Phi_i]^T[m][\Phi_b] & [\Phi_i]^T[m][\Phi_i] \end{bmatrix} \begin{bmatrix} \ddot{\vec{\eta}}_b \\ \ddot{\vec{\eta}}_i \end{bmatrix} + \begin{bmatrix} [\Phi_b]^T[k][\Phi_b] & [\Phi_b]^T[k][\Phi_i] \\ [\Phi_i]^T[k][\Phi_b] & [\Phi_i]^T[k][\Phi_i] \end{bmatrix} \begin{bmatrix} \vec{\eta}_b \\ \vec{\eta}_i \end{bmatrix}$$

$$= \begin{bmatrix} [\Phi_b]^T\vec{f} \\ [\Phi_i]^T\vec{f} \end{bmatrix}$$

or

$$\begin{bmatrix} [M_{bb}] & [M_{bi}] \\ [M_{ib}] & [I_{ii}] \end{bmatrix} \begin{bmatrix} \ddot{\vec{\eta}}_b \\ \ddot{\vec{\eta}}_i \end{bmatrix} + \begin{bmatrix} [K_{bb}] & [0_{bi}] \\ [0_{ib}] & [\Lambda_{ii}] \end{bmatrix} \begin{bmatrix} \vec{\eta}_b \\ \vec{\eta}_i \end{bmatrix} = \begin{bmatrix} \vec{\mathcal{F}}_b \\ \vec{\mathcal{F}}_i \end{bmatrix} \tag{2.12}$$

To obtain frequency response functions for a component modelled by Craig-Bampton coordinates, we may assume harmonic motion of the form

$$\vec{\eta}(t) = \vec{Y} e^{i\Omega t}$$

and let

$$\vec{\mathcal{F}}(t) = \vec{F} e^{i\Omega t}$$

Then,

$$\begin{bmatrix} ([K_{bb}] - \Omega^2 [M_{bb}]) & -\Omega^2 [M_{bi}] \\ -\Omega^2 [M_{ib}] & ([\Lambda_{ii}] - \Omega^2 [I_{ii}]) \end{bmatrix} \begin{bmatrix} \vec{Y}_b \\ \vec{Y}_i \end{bmatrix} = \begin{bmatrix} \vec{F}_b \\ \vec{F}_i \end{bmatrix} \tag{2.13}$$

Assuming that there are only "reaction forces" at the interfaces, that is, that $\vec{F}_i = 0$, then, from the lower row-partition of Eq. (2.13), we get

$$\vec{Y}_i = \Omega^2([\Lambda_{ii}] - \Omega^2[I_{ii}])^{-1}[M_{ib}]\vec{Y}_b \tag{2.14}$$

From the upper row-partition of Eq. (2.13),

$$([K_{bb}] - \Omega^2[M_{bb}])\vec{Y}_b - \Omega^2[M_{bi}]\vec{Y}_i = \vec{F}_b$$

When combined with Eq. (2.14), the above equation becomes

$$[([K_{bb}] - \Omega^2[M_{bb}]) - \Omega^4[M_{bi}]([\Lambda_{ii}] - \Omega^2[I_{ii}])^{-1}[M_{ib}]]\vec{Y}_b = \vec{F}_b \tag{2.15}$$

Alternatively we can write

$$\begin{bmatrix} \vec{Y}_b \\ \vec{Y}_i \end{bmatrix} = \begin{bmatrix} [H_{bb}] & [H_{bi}] \\ [H_{ib}] & [H_{ii}] \end{bmatrix} \begin{bmatrix} \vec{F}_b \\ \vec{F}_i \end{bmatrix}$$

For $\vec{F}_i = 0$, the above expression reduces to

$$\begin{bmatrix} \vec{Y}_b \\ \vec{Y}_i \end{bmatrix} = \begin{bmatrix} [H_{bb}] & [H_{bi}] \\ [H_{ib}] & [H_{ii}] \end{bmatrix} \begin{bmatrix} \vec{F}_b \\ 0 \end{bmatrix}$$

and we have

$$\vec{Y}_b = [H_{bb}]_{Y/F} \vec{F}_b$$

From Eq. (2.15) we obtain the following expression for $[H_{bb}]_{Y/F}$:

$$[H_{bb}]_{Y/F} = [([K_{bb}] - \Omega^2[M_{bb}]) - \Omega^4[M_{bi}]([\Lambda_{ii}] - \Omega^2[I_{ii}])^{-1}[M_{ib}]]^{-1} \qquad (2.16)$$

For simplicity, $[H_{Y/F}]$ will be used in place of $[H_{bb}]_{Y/F}$ for the rest of this discussion. Furthermore, $[H_{Y/F}]$ will be used when the matrix obtained is based on modal coordinates and $[H_{U/F}]$ will be used when the matrix obtained is based on physical coordinates. $[H_{Y/F}]$, which is commonly known as a frequency response function (FRF), is a particular type of transfer function used to express a frequency-dependent ratio of an output motion vector (e.g., displacement) at location a to an applied input force vector at location b. Each element in the FRF matrix is generally complex, but for undamped systems, the elements in the FRF matrix are real. Now, in order to have non-zero "reaction forces" at the interfaces with zero interface displacements, the determinant of $[H_{Y/F}]$ must be zero. This theory is illustrated by a cantilever beam numerical example in Section 2.4.2.

The FRF matrix, $[H_{Y/F}]$, developed here is based on the analytical $[k]$ and $[m]$ matrices. However, a similar $[H^{(e)}_{Y/F}]$ may be generated from modal testing by measuring the displacements at boundary degrees of freedom due to forces applied at boundary degrees of freedom. After the appropriate FRF matrix for a free-boundary test has been generated, the natural frequencies,

damping factors (for damped systems), and mode shapes of the structural system may be extracted from the experimental data using a method such as the polyreference parameter estimation technique[14].

2.4 Numerical Examples - Multiple-Degree-of-Freedom Systems

While the dynamical responses of a few systems with simple geometry, like uniform beams and rods, may be solved using continuous models, most structures must be analyzed using multiple-degree-of-freedom (MDOF) models. Systems with connected particles and/or rigid bodies in general plane motion, and finite element models are examples of MDOF models. In the previous section, a frequency response function matrix of the form $[H_{Y/F}]$ was developed. However, in order to illustrate graphically a relationship between a fixed-boundary test and a free-boundary test, another form of frequency response function matrix might be more helpful. Let us consider a new frequency response function matrix of the form $[H_{F/Y}]$, which is, indeed, $[H_{bb}]^{-1}_{Y/F}$. Similarly, $[H_{F/U}]$ will be used when the matrix obtained is based on physical coordinates. *The main objective of this section is to show that the* **poles** *of* $[H_{F/U}]$ *obtained from a system with free boundaries coincide with the* **natural frequencies** *of the same system with boundaries fixed.* In this matrix, the F's are reaction forces at the boundary degrees-of-freedom, the U's are displacements at the boundary degrees-of-freedom, and the interior forces are zero, that is, $\vec{F}_i = 0$.

2.4.1 A Four-Mass Lumped-Parameter System with Two Interfaces

Consider the following 4-mass system with two boundary degrees-of-freedom, say u_1 and u_2.

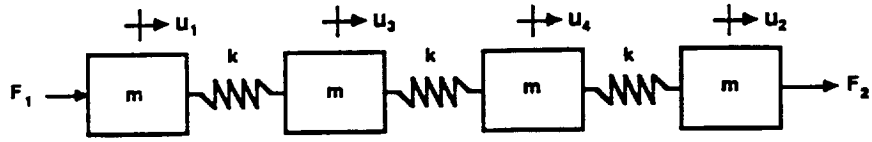

Figure 2.4: Undamped 4-mass system with two interfaces.

The equations of motion for the system in matrix form are

$$\begin{bmatrix} m & 0 & 0 & 0 \\ 0 & m & 0 & 0 \\ 0 & 0 & m & 0 \\ 0 & 0 & 0 & m \end{bmatrix} \begin{bmatrix} \ddot{u}_1(t) \\ \ddot{u}_2(t) \\ \ddot{u}_3(t) \\ \ddot{u}_4(t) \end{bmatrix} + \begin{bmatrix} k & 0 & -k & 0 \\ 0 & k & 0 & -k \\ -k & 0 & 2k & -k \\ 0 & -k & -k & 2k \end{bmatrix} \begin{bmatrix} u_1(t) \\ u_2(t) \\ u_3(t) \\ u_4(t) \end{bmatrix} = \begin{bmatrix} \mathcal{F}_1(t) \\ \mathcal{F}_2(t) \\ 0 \\ 0 \end{bmatrix} \tag{2.17}$$

Assume harmonic motion of the form

$$\vec{u}(t) = \vec{U} e^{i\Omega t}$$

and

$$\vec{\mathcal{F}}(t) = \vec{F} e^{i\Omega t}$$

and substitute these equations into Eq. (2.17) to obtain the harmonic response equation

$$\begin{bmatrix} (1-\lambda) & 0 & -1 & 0 \\ 0 & (1-\lambda) & 0 & -1 \\ -1 & 0 & (2-\lambda) & -1 \\ 0 & -1 & -1 & (2-\lambda) \end{bmatrix} \begin{bmatrix} U_1 \\ U_2 \\ U_3 \\ U_4 \end{bmatrix} = \begin{bmatrix} F_1/k \\ F_2/k \\ 0 \\ 0 \end{bmatrix} \tag{2.18}$$

where $\lambda = m\Omega^2/k$.

When the two boundary degrees-of-freedom of the system are fixed, the above equations of motion may be reduced to

$$\begin{bmatrix} (2-\lambda) & -1 \\ -1 & (2-\lambda) \end{bmatrix} \begin{bmatrix} U_3 \\ U_4 \end{bmatrix} = \begin{bmatrix} 0 \\ 0 \end{bmatrix} \tag{2.19}$$

and the characteristic equation of the clamped-clamped two degree-of-freedom system is

$$\lambda^2 - 4\lambda + 3 = 0 \tag{2.20}$$

Next, assume that the system is free. Thus, we can express the "reaction forces," F_1 and F_2, in terms of U_1 and U_2 using Eq. (2.18). The result, in matrix form, is given by

$$\begin{bmatrix} F_1/k \\ F_2/k \end{bmatrix} = -\frac{1}{(\lambda^2 - 4\lambda + 3)}[A] \begin{bmatrix} U_1 \\ U_2 \end{bmatrix} \tag{2.21}$$

where

$$[A] = \begin{bmatrix} (\lambda^3 - 5\lambda^2 + 6\lambda - 1) & 1 \\ 1 & (\lambda^3 - 5\lambda^2 + 6\lambda - 1) \end{bmatrix}$$

Now, in order to have non-zero "reaction forces" with zero displacements at the interfaces, the following condition must be satisfied.

$$\lambda^2 - 4\lambda + 3 = 0 \tag{2.22}$$

Note that Eqs. (2.20) and (2.22) give the same result. This simple example illustrates the fact that the poles of $[H_{F/U}]$ obtained from a system with free boundaries coincide with the natural frequencies of the same system with boundaries fixed.

2.4.2 Undamped Finite Element Models

In most instances, finite element models, rather than lumped-parameter models, are used to describe the dynamic behavior of structures. In many instances when the original system is too large or has too many degrees-of-freedom, it is necessary to use some kind of model reduction method such as the component mode synthesis method discussed in Section 2.2. The theory derived in Sections 2.2 and 2.3 are based on modal coordinates and will now be applied to a numerical example to show, as in Section 2.4.1, that the *poles* of frequency response function matrix, $[H_{F/Y}]$, for a system with free boundaries are the same as the *natural frequencies* of the same system with boundaries fixed.

Dynamical responses of simple structural members based on finite element representation of the members will now be illustrated. The transverse vibration of a uniform cantilever beam will be used for this purpose. The Craig-Bampton coordinates outlined in Section 2.2 will be used to define the structural components. Computer software packages ISMIS[15] and PC-MATLAB[16] will be used to generate the necessary system parameters and to perform response simulation of the mathematical model, respectively. Additional examples are provided in Reference[1].

Consider the transverse vibration of the 4-element cantilever beam in Fig. 2.5. Figure 2.5(a) displays all 15 degrees-of-freedom before reduction. After applying the conditions that the right hand end of the beam is fixed and that the axial freedom is restricted, the number of degrees of freedom of the system reduces to eight, as shown in Fig. 2.5(b).

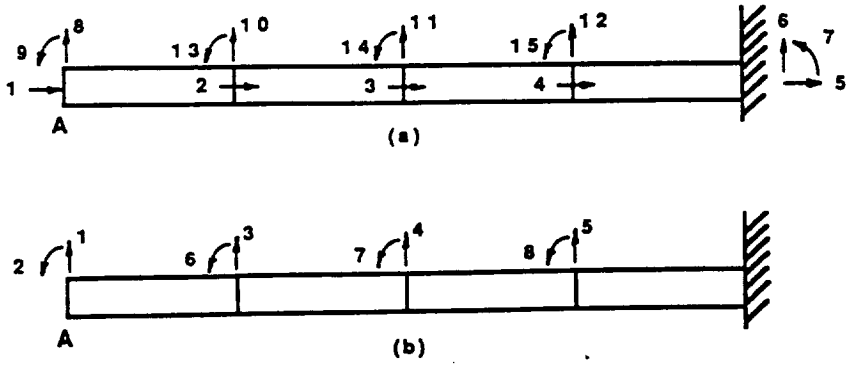

Figure 2.5: A four-element cantilever beam. (a) The coordinates before reduction. (b) The coordinates after reduction.

Based on Craig-Bampton coordinates, degrees-of-freedom 1 and 2 will be treated as boundary degrees of freedom and will be defined using constraint modes. The rest of the degrees of freedom will be treated as interior degrees of freedom and will be defined using fixed-interface normal modes. Material properties used in this analysis are : $E = 10.0 \times 10^6$ psi, $I = 8.333 \times 10^{-2}$ in^4, $A = 1$ in^2, and $\rho = 2.591 \times 10^{-4}$ lb s^2/in^4.

Figures 2.6 through 2.9 show the frequency response functions $(H_{F/Y})_{11}$, $(H_{F/Y})_{12}(= (H_{F/Y})_{21})$, and $(H_{F/Y})_{22}$ for the system. These are actually dynamic stiffness plots, for they are plots of "reaction forces" over displacements at the interface, A. (This is also the reason why there are *more* zeros than poles in the plots.) These plots are obtained with the interface free and with the forces applied at interface degrees of freedom to keep them from moving, while the rest of the beam undergoes transverse vibration. Figure 2.9 is an overlay of Figs. 2.6 through 2.8, and it shows that the poles in all three plots correspond to the same frequencies. These are the forcing frequencies at which the beam must be excited in order to obtain non-zero "reaction forces" with

zero displacements at the interface. Since there are six interior degrees-of-freedom, there are six poles in the figure. For easy reference, the values of the six poles are tabulated in Table 2.1 below. Values in the first column are obtained for the cantilever beam with end A fixed. These values correspond to the natural frequencies for a clamped-clamped beam. On the other hand, the values in the second column are obtained for the cantilever beam with end A free. The percentage errors for the frequencies are essentially roundoff errors

Table 2.1: Undamped natural frequencies for the cantilever beam example (rad/s).

Fixed-Interface Frequencies ($\times 10^4$)	Poles of $[H_{F/Y}]$ ($\times 10^4$)	% Error
0.079388	0.079378	0.013
0.220615	0.220683	0.031
0.437689	0.437679	0.002
0.828066	0.828019	0.006
1.369499	1.369407	0.007
2.206608	2.206574	0.002

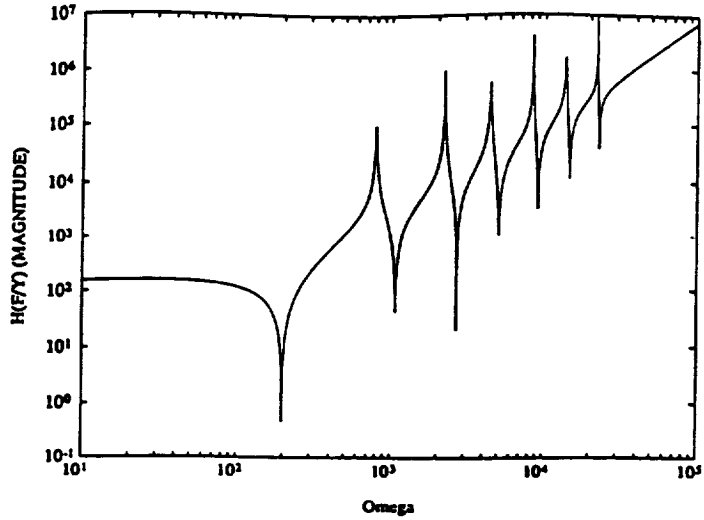

Figure 2.6: Frequency response function $(H_{F/Y})_{11}$ for cantilever beam example.

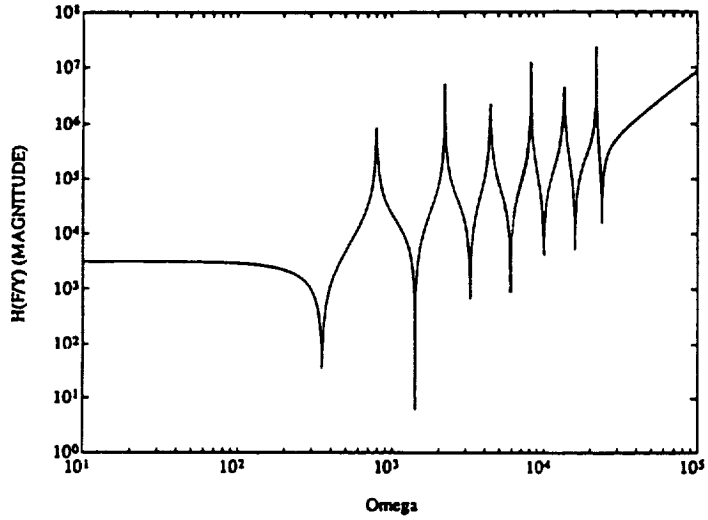

Figure 2.7: Frequency response function $(H_{F/Y})_{12} = (H_{F/Y})_{21}$ for cantilever beam example.

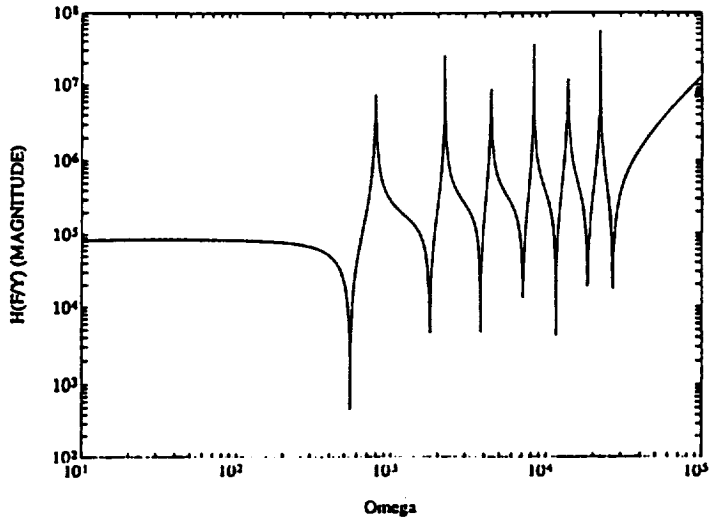

Figure 2.8: Frequency response function $(H_{F/Y})_{22}$ for cantilever beam example.

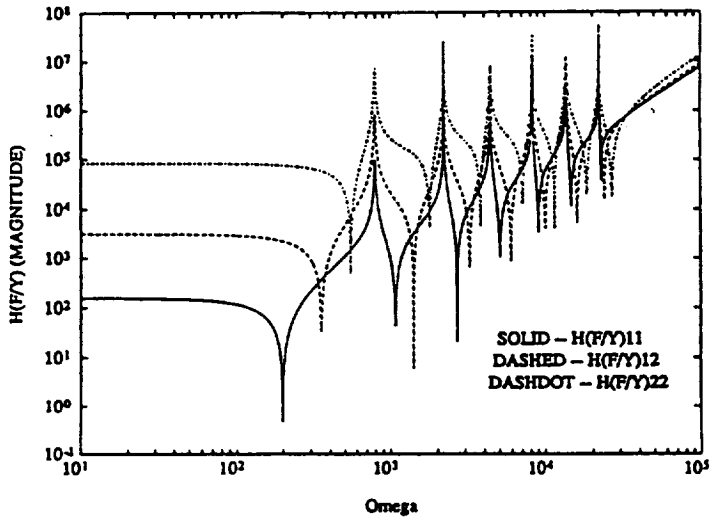

Figure 2.9: Frequency response function for cantilever beam example.

2.5 Numerical Examples - Undamped Continuous Systems

All physical structures are, in fact, three-dimensional and, if unrestrained, capable of translating in the x-, y-, z-directions and rotating about the mutually perpendicular x-, y-, z-axes. Although the verification theories discussed in Section 2.3 are expressed in a "discretized" form, they are, indeed, also applicable to continuous systems. In the following example, we will show that the *zeros* of determinant of the frequency response function matrix of the form $[H_{U/F}]$ obtained from a system with free boundaries coincide with the *natural frequencies* of the same system with boundaries fixed. To relate the example in this section to the previous examples, we will also show that the *poles* of frequency response function matrix $[H_{F/U}]$ obtained from a system with free boundaries coincide with the *natural frequencies* of the same system with boundaries fixed. Additional examples are provided in Ref.[1].

2.5.1 Transverse Vibration of Linearly Elastic Beams - Fixed-Boundary Approach

A case having more than one interface boundary constraint will now be examined. Consider the free vibration of a Bernoulli-Euler beam pinned at both ends, as shown in Fig. 2.10.

The equation of motion for this system is given by

$$(EIv'')'' + \rho A\ddot{v} = 0 \tag{2.23}$$

where E is the modulus of elasticity, I is the area moment of inertia, and A is the cross-sectional area of the beam.

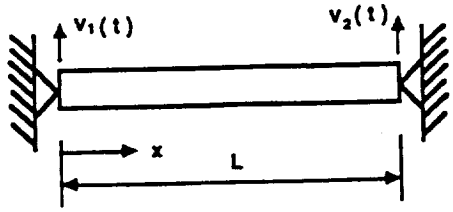

Figure 2.10: A pinned Bernoulli-Euler beam in transverse vibration.

Assume a harmonic motion of the form

$$v(x,t) = V(x)\cos(\omega t) \tag{2.24}$$

where ω is the undamped natural frequency. Substitute this into Eq. (2.23) to obtain the differential eigenproblem

$$(EIV'')'' - \rho A\omega^2 V = 0 \tag{2.25}$$

In order to obtain a closed-form solution, the beam is assumed to be uniform, that is, $EI = const.$, $\rho A = const.$. Then,

$$\frac{d^4V}{dx^4} - \lambda^4 V = 0 \tag{2.26}$$

where

$$\lambda^4 = \frac{\rho A\omega^2}{EI}$$

The general solution for Eq. (2.26) is given by

$$V(x) = C_1\sinh(\lambda x) + C_2\cosh(\lambda x) + C_3\sin(\lambda x) + C_4\cos(\lambda x) \tag{2.27}$$

The boundary conditions to be used are

$$\begin{array}{lll} V(0) = 0 & , & EIV''(0) = 0 \\ V(L) = 0 & , & EIV''(L) = 0 \end{array} \tag{2.28}$$

From Eqs. (2.27) and (2.28), the characteristic equation for the system is obtained

$$\sin(\lambda_r L)\sinh(\lambda_r L) = 0 \tag{2.29}$$

This equation determines the natural frequencies of the beam with pinned ends ("fixed" against translation).

2.5.2 Transverse Vibration of Linearly Elastic Beams - Free-Boundary Approach

We will next consider the forced vibration of a free-free Bernoulli- Euler beam with a sinusoidal excitation on the right-hand end of the beam as shown in Fig. 2.11.

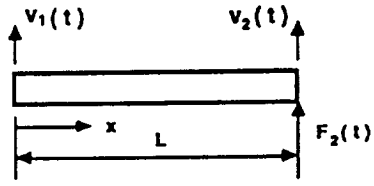

Figure 2.11: A free-free beam in transverse vibration.

The appropriate equation for the above system is again Eq. (2.25), but

the boundary conditions are now

$$\begin{array}{lll} EIV''(0) = 0 & , & EIV'''(0) = 0 \\ EIV''(L) = 0 & , & EIV'''(L) = -F_2 \end{array} \tag{2.30}$$

Let the forcing frequency (rad/sec) be Ω, and let $\beta^4 = \frac{\rho A \Omega^2}{EI}$. From Eq. (2.27) (with β replacing λ) and Eqs. (2.30), the transverse displacement of the right-hand end of the beam is found to be

$$V_2 \equiv V(L) = -\frac{F_2[\sin(\beta L)\cosh(\beta L) - \cos(\beta L)\sinh(\beta L)]}{EI\beta^3[1 - \cos(\beta L)\cosh(\beta L)]}$$

and a frequency response function of the form, H_{V_2/F_2}, can be written as

$$H_{V_2/F_2} \equiv H_{22} = -\frac{\sin(\beta L)\cosh(\beta L) - \cos(\beta L)\sinh(\beta L)}{EI\beta^3[1 - \cos(\beta L)\cosh(\beta L)]} \tag{2.31}$$

Similarly, the transverse displacement of the left-hand end of the beam is found to be

$$V_1 \equiv V(0) = -\frac{F_2[\sin(\beta L) - \sinh(\beta L)]}{EI\beta^3[1 - \cos(\beta L)\cosh(\beta L)]}$$

and a frequency response function of the form, H_{V_1/F_2}, can be written as

$$H_{V_1/F_2} \equiv H_{12} = -\frac{\sin(\beta L) - \sinh(\beta L)}{EI\beta^3[1 - \cos(\beta L)\cosh(\beta L)]} \tag{2.32}$$

Based on the symmetry of the problem, the following results are also true.

$$H_{V_1/F_1} \equiv H_{11} = -\frac{\sin(\beta L)\cosh(\beta L) - \cos(\beta L)\sinh(\beta L)}{EI\beta^3[1 - \cos(\beta L)\cosh(\beta L)]} \tag{2.33}$$

and

$$H_{V_2/F_1} \equiv H_{21} = -\frac{\sin(\beta L) - \sinh(\beta L)}{EI\beta^3[1 - \cos(\beta L)\cosh(\beta L)]} \tag{2.34}$$

Expressions (2.31) through (2.34) may then be expressed in a matrix form as

$$\begin{bmatrix} V_1 \\ V_2 \end{bmatrix} = \begin{bmatrix} H_{11} & H_{12} \\ H_{21} & H_{22} \end{bmatrix} \begin{bmatrix} F_1 \\ F_2 \end{bmatrix} \tag{2.35}$$

One very important thing to note at this point is that the frequency response function matrix, $[H]$, is obtained based on a free-free condition. Now, for a beam with both ends pinned, we have $V_1 = V_2 = 0$, then

$$\begin{bmatrix} 0 \\ 0 \end{bmatrix} = \begin{bmatrix} H_{11} & H_{12} \\ H_{21} & H_{22} \end{bmatrix} \begin{bmatrix} F_1 \\ F_2 \end{bmatrix}$$

In order to have a non-zero reaction force at the interfaces, the determinant of $[H]$ must be zero, thus

$$\begin{vmatrix} H_{11} & H_{12} \\ H_{21} & H_{22} \end{vmatrix} = 0$$

or

$$H_{11}H_{22} - H_{12}H_{21} = 0 \tag{2.36}$$

After some algebraic manipulations with Eqs. (2.31) through (2.34) and (2.36), we obtain

$$\sin(\beta L)\sinh(\beta L) = 0 \tag{2.37}$$

Equations (2.29) and (2.37) are identical if $\beta = \lambda_r$.

The analysis shows that instead of a fixed-boundary test, which is difficult to simulate, the same information can be obtained from a free-free test regardless of the number of interfaces involved. Hence, for a system with more than one interface, first we need to determine all the elements of the frequency response function matrix, $[H_{U/F}]$, i.e., H_{ij}, i = 1,...,n; j = 1,...,n; where n is the total number of interfaces. It will be helpful to remember that $H_{ij} = H_{ji}$. Once the full matrix has been generated, we can then take the determinant of the said matrix and set it to zero to extract the *zeros* for the free-free system.

Similarly, a frequency response function matrix of the form, $[H_{F/U}]$, may be obtained for this system with multiple interfaces. From Eq. (2.35), we obtain

the following expressions

$$V_1 = H_{11}F_1 + H_{12}F_2$$
$$V_2 = H_{21}F_1 + H_{22}F_2$$

Solving the above expressions for F_1 and F_2 in terms of V_1 and V_2 gives

$$\begin{bmatrix} F_1 \\ F_2 \end{bmatrix} = \frac{1}{H_{11}H_{22} - H_{12}H_{21}} \begin{bmatrix} H_{22} & -H_{12} \\ -H_{21} & H_{11} \end{bmatrix} \begin{bmatrix} V_1 \\ V_2 \end{bmatrix} \tag{2.38}$$

Note that the denominator expression of Eq. (2.38) is identical to Eq. (2.36). Hence, the *poles* of frequency response function matrix $[H_{F/U}]$ obtained for systems with free boundaries coincide with the *natural frequencies* of the same systems with boundaries fixed.

2.6 Remarks and Conclusions

Due to the difficulty in simulating a fixed-base modal test, an alternative in the form of a free-suspension test is investigated in Ref.[1]. It is found that the *poles* of each element of a frequency response function matrix, $[H_{F/U}]$, obtained for a system with free boundaries coincide with the *natural frequencies* of the same system with boundaries fixed.

However, in practical experimental analysis, a frequency response function matrix of the form $[H_{U/F}]$ may be generated more readily than $[H_{F/U}]$. A similar relationship between the fixed-base and free-suspension systems may be discovered after taking the determinant of $[H_{U/F}]$ and setting the resulting polynomial to zero. For cases where the determinant may be expressed explicitly in a fractional form, the *zeros* in such cases coincide with the *natural frequencies* of the fixed-base system. In other cases where the determinant may only be expressed in a polynomial form, the *frequencies* corresponding to

a zero magnitude of the determinant coincide with the *natural frequencies* of the fixed-base system.

Several additional topics are also addressed in Ref.[1], namely how the theory illustrated above is affected if the system has closely-spaced frequencies, and whether mass and stiffness perturbations ("errors") have a significant effect on the FRF's studied.

The possibility of repeated eigenvalues in a given system has also been addressed in Ref.[1]. These eigenvalues can be identified from the determinant plot of $[H_{U/F}]$ using a Sturm sequence approach; they show up as a "flattening" in the plot. The more times a certain eigenvalue is repeated, the flatter will be the curve at that frequency location.

A simple error analysis has been conducted on an undamped 4-mass system by varying element stiffness and mass parameters. Results for this analysis indicate that for an arbitrary mass perturbation, variation in eigenvalues increases for higher stiffness and that for an arbitrary stiffness perturbation, variation in eigenvalues increases for lighter mass. A second error analysis has been conducted on an undamped 15-component clamped-clamped beam by varying the modulus and area of individual components. Results for varying individual component modulii by 2% indicate that the number of components displaying higher percentage change in eigenvalues increases for higher modes. Furthermore, the effect of first and last components on eigenvalue variations decreases for higher modes. Similarly, results for varying individual component areas by 2% indicate that the number of components displaying higher percentage change in eigenvalues increases for higher modes. However, the effect of first

and last components on eigenvalue variations increases for higher modes. For a more conclusive deduction, an extensive study using perturbation theories should be carried out in the future to assist in isolation of modeling errors and updating of mathematical models.

Finally, the material presented in Ref.[1] is purely analytical, so the theory developed and illustrated by numerical simulations should be applied to a physical system in a modal test to assess their usefulness.

Chapter 3

A REVIEW OF ERROR LOCALIZATION AND MODEL UPDATING FOR STRUCTURAL COMPONENTS (REF.2)

This report consists of detailed reviews of the major published methods available for locating modeling errors and for updating mathematical models, e.g. finite element models, by the use of modal test data. This review of literature was conducted under the present grant, NASA grant NAG 9-346. The report also contains the result of numerical evaluations of the methods when applied for a simplified payload–test-stand simulation. This latter work was supported by NASA grant NAG 9-484.

From the structures standpoint, the most important question to be asked in creating a mathematical model for use in a structural dynamics study is, "What is the purpose of the model?" Due to the size and complexity of present day aerospace structures, and due to the limited amount of computer resources available, the structural dynamicist must be able to represent an original structural system model by a much reduced set of degrees of freedom.

The basic mathematical (or analytical) model is constructed in accordance with assumptions concerning the distribution of mass and stiffness, with damping usually neglected. The resulting model may, or may not, be reasonably representative of the actual structure, and the inaccuracies present in the analytical model may be due to the approximation of boundary conditions, to

the estimation of material properties, to the lack of damping representation, and so forth.

In spite of such common shortcomings, the advantages of an analytical model over an experimental model are evident. In addition to low cost, the analytical model can be modified during the design stage to optimize the dynamic behavior of the structure without need for a prototype. But the uncertainties inherent in the analytical modelling technique make model verification a necessity. Therefore, it is absolutely essential for some form of dynamic testing to be performed to verify the analytical models.

Substructuring, also referred to as component mode synthesis (CMS), is frequently used for analyzing the dynamics of aerospace structures. This is due to the fact that components of an aerospace system (e.g., the Space Shuttle Orbiter plus payloads) are frequently designed by different engineering contractors, so there exists a need for communication and assembling accurate component models of reasonable order. Furthermore, dynamic analysis and testing may be required on system configurations comprised of different collections of components.

Reviewing the history of CMS studies, we note that several different methods exist for the representation of a component substructure for the purpose of system component mode synthesis. These methods are categorized by the way the interface degrees of freedom are treated during the computation of component normal modes. The four basic categories of CMS are: 1) fixed-interface methods, 2) free-interface methods, 3) loaded-interface methods, and 4) hybrid-interface methods.

Usually, a modal test is performed to measure the modal parameters. The measured natural frequencies can be compared relatively easily with the calculated ones because these are scalars. As the mode shapes are vectors, the comparison is more difficult. To address this problem, there are a number of checks, such as orthogonality and cross-orthogonality checks, the modal assurance criterion, and visualization of the difference between measured and analytical mode shapes.

In general, the analytical model will have more degrees of freedom than the test configuration will have accelerometers. In order to carry out these checks, the number of analytical degrees of freedom has to be reduced or the number of measured degrees of freedom has to be extended.

Often differences are observed between the experimental and analytical results. These differences may be due to experimental errors or due to errors in the analytical model. Experimental errors may result from wrong measurements, influence of test equipment on the test structure, mismatch of boundary conditions between the analytical model and the test set-up, and so forth.

In recent years many methods have been developed to localize errors in the analytical model and to update the analytical model through the use of vibration test data. The process of adjusting the analytical model to match test results is called system identification and model updating.

Reviewing the history of system identification and model updating studies, we can see that there are basically two major categories currently in use. In the first category, error localization, the task is to localize the major modelling errors, rather than to update directly. In the second category, model updating,

the task is to seek a new model that is mathematically optimal and that satisfies certain physical constraints. In general, statistical parameter estimation, direct matrix updating, and nonlinear programming optimization updating are three common ways that are used for model updating. Physical parameters (such as ρ, E, I) are updated in statistical parameter estimation and nonlinear programming updating techniques, whereas, in direct matrix updating techniques, system or element mass and stiffness matrices are corrected.

A Space Shuttle payload is treated as a component whose math model is to be interfaced with an orbiter math model. Space Shuttle payload tests have been conducted with fixed interface supports, with free interfaces and with loaded interfaces. Validation of the analytical model in the vicinity of the payload/orbiter interfaces is crucial. The analytical model must accurately represent the boundary conditions of the test article in order to obtain an acceptable correlation. Therefore, a fixed-interface analytical model cannot be updated directly by using free-interface test results.

In this report, recent error localization and model updating methods are reviewed, but the topics of types of analytical and experimental models, reconciliation of degrees of freedom of analytical and experimental models, and correlation between analytical model prediction and modal test data are not included.

3.1 Error Localization

The primary purpose of the error localization approach is to improve an analytical model by attempting to locate modelling errors in the model using

the limited information obtained from an experimental model. This is based on the assumption that the major modelling errors in the analytical model are often isolated rather than distributed, therefore any attempt to correct the whole analytical model is inefficient.

There are several researchers working on this subject. Ewins proposed the Error Matrix Method (EMM) to locate analytical mass and stiffness matrix errors by using a binomial expansion[17]. Later, he used Singular Value Decomposition (SVD) to calculate error matrices[18]. These error matrices indicate not only where the differences exist between experimental and analytical models, but the absolute magnitudes of the errors are also indicated.

The Force Balance Method was proposed by Fissette and Ibrahim [19]. This is based on implementing the dynamic equation, and the elements that possess a high unbalanced force need to be updated. Lin proposed the Unity Check Method to determine an analytical stiffness error matrix[20]. This method uses the cross unity check between the flexibility matrix derived from the experimental model and the stiffness matrix of the analytical model to locate errors. Unlike EMM, the error matrices obtained by the Fissette method or the Lin method indicate only where the modelling differences exist between the experimental model and the analytical model.

Chou, O'Callahan, and Wu present a new procedure that is used to spatially localize the experimental and analytical model errors using the structural element connectivity in the model space[21]. Like EMM, the model error matrices obtained by the O'Callahan method indicate not only the modelling differences between the experimental and analytical models, but also the ab-

solute amplitudes of the errors. Therefore, the corrected system matrices in the physical space may then be generated by assembling the spatially-corrected element mass and stiffness matrices.

In the following sections the above methods will be briefly described.

3.1.1 The Error Matrix Method

The basic theory of the Ewins' Error Matrix Method[17] is to compute the differences of experimental/analytical stiffness and mass matrices by use of a binomial expansion or by a singular value decomposition.

Binomial Expansion Technique

First, we will discuss the binomial expansion approach. To begin with the stiffness case, EMM first assumes that a complete and correct experimental stiffness matrix, K_t, exists as well as the incorrect analytical one, K_a. (In reality K_t does not exist, but its inverse may be estimated through measured mode shapes and frequencies.) Then EMM defines the difference between K_t and K_a as the stiffness error matrix ΔK:

$$\Delta K = K_t - K_a \tag{3.1}$$

Rearranging and inverting both sides gives

$$K_t^{-1} = (K_a + \Delta K)^{-1} = (I + K_a^{-1}\Delta K)^{-1} K_a^{-1} \tag{3.2}$$

It can be shown[17] that, by ignoring the second and higher-order terms in the binomial expansion of a matrix inverse, the error matrix ΔK can be approximated as

$$\Delta K \approx K_a(K_a^{-1} - K_t^{-1})K_a. \tag{3.3}$$

The two "pseudo-flexibility" matrices can be estimated using the corresponding modal data, so that Eq.(3.3) becomes

$$\Delta K \approx K_a(\Phi_a \Omega_a^{-2} \Phi_a^T - \Phi_t \Omega_t^{-2} \Phi_t^T) K_a. \tag{3.4}$$

where

$$\begin{aligned} \Phi_a &= \text{analytical mode shape matrix} \\ \Omega_a &= \text{analytical diagonal frequency matrix} \\ \Phi_t &= \text{experimental mode shape matrix} \\ \Omega_t &= \text{experimental diagonal frequency matrix.} \end{aligned}$$

In general, all matrices in Eq.(3.4) are assumed to be of full order (i.e., $N \times N$), but there also could be an incomplete set of modes, say m, so that Φ_a and Φ_t are $N \times m$, and Ω_a and Ω_t are $m \times m$.

In practice, the number of degrees of freedom in the experimental model, say n, is less than that of the analytical model, say N ($n < N$). In order to estimate the error matrix in Eq.(3.4), the analytical model must be reduced or the experimental mode shapes must be expanded. In the case of reducing the analytical model, Eq.(3.4) becomes

$$\Delta K^R \approx K_a^R(\Phi_a \Omega_a^{-2} \Phi_a^T - \Phi_t \Omega_t^{-2} \Phi_t^T) K_a^R. \tag{3.5}$$

where mode shape matrices Φ_a and Φ_t are now of order $n \times m$, and superscript R denotes a reduced analytical model. In a similar manner, the mass error matrix between the correct experimental mass matrix, M_t, and the incorrect analytical mass matrix, M_a is [22]

$$\Delta M^R \approx M_a^R(\Phi_a \Phi_a^T - \Phi_t \Phi_t^T) M_a^R. \tag{3.6}$$

Singular Value Decomposition Technique

In Ref.[18], Lieven and Ewins presented a new method using singular value decomposition (SVD) to take the pseudo inverse of rank-deficient matrices, which are known as the flexibility and inertance matrices, for both the analytical and experimental systems. The SVD method is described in detail in Ref.[2].

3.1.2 The Force Balance Method

The force balance method proposed by Fissette and Ibrahim [19] is based on the unbalanced forces of the dynamic system that result from the discrepancies between the analytical model and the experimental model. It is assumed that the test data are correct and that only the analytical stiffness matrix needs to be updated (i.e., the analytical mass matrix is also correct).

From the dynamic system, we have

$$(K_a - \Omega_{t_i}^2 M_a)\Phi_{t_i} = E_i \tag{3.7}$$

where E_i is the ith error vector or simply the ith vector of unbalanced forces, and Ω_{t_i}, Φ_{t_i} represents the ith test frequency and mode shape. By defining $D_{r_i} \equiv K_a - \Omega_{t_i}^2 M_a$, then Eq.(3.7) becomes

$$D_{r_i}\Phi_{t_i} = E_i \tag{3.8}$$

It can be seen from Eq.(3.8) that if i^{th} row of D_{r_i} is zero, then the i^{th} element of E_i is also zero. Equation (3.8) shows that the magnitude of such unbalanced forces is different from one mode to another. However, the

distribution of the unbalanced forces should be the same, and it is expected to correspond to the degrees of freedom where modelling errors exist. This error vector, E_i can be graphically displayed to show the matrix regions where discrepancies are found, and this type of information is useful to identify areas in the analytical model that need further updating.

If we use more than one mode, then Eq.(3.8) can be written in matrix form as

$$D_r \Phi_t = E \tag{3.9}$$

For further applications of this method, see Ref.[19].

3.1.3 The Unity Check Method

In this approach to locating modelling error, Lin [20] assumed that the test data and the analytical mass matrix are correct. The method checks the deviation from unity of the product of the flexibility matrix derived from test data and the analytical stiffness matrix.

If the measured modes and frequencies are assumed to be accurate, the analytical stiffness matrix will also be accurate if the following unity condition is satisfied

$$F_t K_a = I \tag{3.10}$$

where I is a unity matrix and F_t is the flexibility matrix of the experimental model; otherwise K_a is in error. In general, the stiffness matrix is banded or has strong diagonal terms. Thus, local modelling errors will significantly affect only those stiffness coefficients directly connected to or closely related to erroneously modeled areas. These affected stiffness coefficients will influence

only columns associated with the affected degree of freedom in the product of F_t and K_a.

Physically, each column of K_a represents a set of nodal forces due to a unit displacement at one degree of freedom while others are held fixed. From Eq.(3.10), the difference of the product of $F_t K_a$ and the unity matrix, I, can be expressed by an error matrix E defined as follows:

$$E = F_t K_a - I \tag{3.11}$$

The maximum absolute value of elements in the corresponding column of E indicates the error for each degree of freedom, that is

$$e_j = \max_i |e_{ij}| \tag{3.12}$$

where the $e_{ij}{}'s$ are the elements of E. An e_j is a measurement of deflection errors caused by errors in the jth column of K_a. A large value of e_j indicates the j^{th} degree of freedom is affected by modelling errors. Equation (3.11) can be described by another form

$$E = (F_t - F_a)K_a \tag{3.13}$$

Finally, as in Eq.(3.4), we have the following equation

$$E = (\Phi_t \Omega_t^{-2} \Phi_t^T - \Phi_a \Omega_a^{-2} \Phi_a^T) K_a \tag{3.14}$$

A complete set of modes, or only the lower modes, can be used in Eq.(3.14) to identify modelling errors. Note that Eq.(3.14) is a transposed form of the method proposed by Ojalvo and Pilon [23]

3.1.4 The Structural Element Connectivity Method

Chou, O'Callahan and Wu[21] proposed a new method to spatially localize the experimental/analytical model errors using a least-squares approach in modal space. After the system error stiffness and mass matrices are generated, the updated stiffness and mass matrices may also be obtained.

The eigenequations of motion for an undamped n degree of freedom system can be written as

$$K_a \Phi_a = M_a \Phi_a \Omega_a^2 \tag{3.15}$$

where Φ_a is the order $n \times m$ modal matrix containing m mode shapes as columns. The diagonal elements in Ω_a^2 are the corresponding squared natural frequencies. The system mass matrix M_a $(n \times n)$ is an assembly of the element mass matrices $M_{a_i}(n \times n)$

$$M_a = \sum_i M_{a_i} = \sum_i C_i^T m_{a_i} C_i \tag{3.16}$$

where C_i $(e \times n)$ is the ith element connectivity matrix relating the ith element mass matrix m_{a_i} $(e \times e)$ to the system physical degrees of freedom. The system stiffness matrix K_a $(n \times n)$ can also be expressed as an assembly of its individual elements.

$$K_a = \sum_i K_{a_i} = \sum_i C_i^T k_{a_i} C_i \tag{3.17}$$

If errors exist in the analytical model, and the experimental modal matrix, Φ_t, and the squared natural frequency matrix, Ω_t^2, are assumed to be accurate, then a new eigensolution for the system may be expressed as

$$(K_a + \Delta K)\Phi_t = (M_a + \Delta M)\Phi_t \Omega_t^2 \tag{3.18}$$

Finally, the modified system mass and stiffness matrices in the physical space can be generated by assembling the element modal error matrices, that is,

$$\Delta M = \sum_i C_i^T \Delta m_{a_i} C_i \tag{3.19}$$

$$\Delta K = \sum_i C_i^T \Delta k_{a_i} C_i \tag{3.20}$$

The procedure for evaluating the element modal error matrices Δm_{a_i} and Δk_{a_i} is described fully in Refs.[21] and [2].

3.2 Model Updating

In addition to error localization, much research effort is being devoted to the topic of model updating. Statistical estimation, direct model updating, and nonlinear programming optimization are the updating techniques generally used.

Collins, et.al.[24] first formulated a statistical parameter estimation technique in an iterative procedure for systematically using measured natural frequencies and mode shapes of a structure to modify the stiffness and mass characteristics of an analytical model. Instead of directly improving the analytical stiffness and mass matrices, this techniques seeks to modify the physical parameters or design variables (such as, E, I, ρ) of an analytical model. Although this method preserves the connectivity of the original analytical model during the iteration, the application of this method to real structures is restricted because its formulation is complex.

The statistical parameter estimation technique has its merits; for example, all operations are performed with the full finite element model. This

provides the information on structure parameter changes required for improving the analytical model. However, since all operations are performed using the full model, computational requirements may be very high. Thus, it is important that only a relatively few iterations be needed for updating.

CORDS[25] is a computer code developed by the Structural Dynamics Research Corporation (SDRC). It is based on the use of design sensitivity calculations and optimization to minimize the difference between the test and analysis results. Design sensitivity data is used to predict the effects of small changes about the current design point. The objective of the optimization process is to identify optimum sets of changes that minimize the error between test and analysis results with minimum changes to the model. This process is used in an iterative manner and results in rapid and uniform improvement of test/analysis correlation with reasonable changes to the model.

For direct updating, Berman and Flannely[26] presented a method for identifying parameters in a linear, discrete model of a structure by using incomplete measured normal modes to modify an analytical model. Later, Baruch and Itzhack[27] presented a method to obtain an optimal orthogonalization of measured mode shapes. The method is based on the assumption that the analytical mass matrix is accurately known and that the measured natural frequencies are accurate. The orthogonalized modes are used to optimally correct the analytical stiffness matrix.

Baruch[28] employed two different versions for updating the analytical model. In both versions, measured mode shapes are assumed to be accurate. In the first version, the mass matrix, which is considered to be known with

higher confidence, is corrected to meet the orthogonality conditions, and then the stiffness matrix is corrected to satisfy the dynamic equations. In the second version, the stiffness matrix, which is now considered to be known with higher confidence, is corrected to meet the orthogonality conditions, and then the mass matrix is corrected to satisfy the dynamic equation.

Besides the measured mode shapes and the analytical mass matrix considered as the reference basis, Baruch[28] also proposed the analytical stiffness matrix as a reference basis to modify the mode shape and the analytical mass matrix. In the above three methods, Lagrange multipliers are used and a closed-form solution is obtained.

Berman and Nagy[29] applied constrained optimization theory by using measured mode shapes and natural frequencies to improve the analytical mass and stiffness matrices of a structure. In this approach, measured mode shapes are assumed to be accurate, and the standard Lagrange multiplier method is used to solve the optimization problem. Chen and Fu[30], and O'Callahan and Leung[31], respectively, employed a generalized inverse technique on the measured mode shapes to optimize the analytical mass and stiffness matrices. The result is the same as in Ref.[29].

Chen, et.al.[32, 33] introduced a matrix perturbation theory in which the correct mass and stiffness matrices are expanded in terms of analytical values plus a modification matrix.

The Error Matrix Method by Ewins (see Sec.3.1.1) also may be considered as a direct updating method. The error matrices computed by EMM indicate not only the modelling differences between the analytical and exper-

imental models, but also the absolute magnitudes of the errors. Therefore, the error matrices may be added to original erroneous analytical mass/stiffness matrices to obtain corrected mass/stiffness matrices.

For the direct updating described above, the structure connectivity is always destroyed. Therefore, Kabe[34] proposed to apply structural connectivity information to optimally adjust an incorrect analytical stiffness matrix. The percentage change to each stiffness coefficient is minimized, and the physical configuration of the analytical model is preserved.

Wei[35, 36] derived an element correction method to modify the analytical dynamic model. This method employs the structural connectivity to correct the mass and stiffness matrices simultaneously, while enforcing the orthogonality and dynamic equation constraints.

A Linear Quadratic Optimization (LQO) theory containing linearization and solution of the conventional matrix optimization problem is proposed by Lapierre and Ostiguy[37]. It ensures that the original connectivity condition of the structure analyzed is preserved during the updating process.

The methods of Kabe, Wei and Lapierre, which attempt to preserve the structural connectivity condition, are all based on preserving the zero and non-zero character of terms of the stiffness matrix. However, connectivity constraints based solely on a zero/non-zero element pattern of a stiffness matrix can be misleading. Certain zero elements in a stiffness matrix result from cancellations of the stiffness properties of similar structure elements that do possess physical connectivity. The actual structural node connectivity obtained during the FEM assembly process should be used to constrain the system error

matrices.

Like EMM, the model error matrices obtained by the O'Callahan method [21] indicate not only modelling differences between experimental and analytical models but absolute amplitudes of the errors. This method is used to spatially localize the experimental/analytical model errors using the structural element connectivity in the model space. Also, the corrected system matrices in the physical space may then be generated by assembling the spatially corrected element mass and stiffness matrices. Details of this method may be seen in Sec.3.1.4.

Besides the many updating techniques described above, there are some researchers working on model updating by the use of nonlinear programming techniques. Janter, Heylen and Sas[38] proposed the UA (User Acceptance) model updating scheme that is based on enabling a user to formulate mathematically his ideas and experience of what an acceptable model should be.

Reference [2] contains a detailed description of the statistical estimation update procedure of Ref.[24]. The direct model updating procedures of Berman and Nagy[29]; Baruch and Bar Itzhack[27]; Chen and Fu[30]; O'Callahan and Leung[31]; Chen, Kuo, and Garba[33]; and Kabe[34] are described in detail in Ref.[2]. Here, the details of the design sensitivity update procedure of Ref.[25] are given to illustrate one approach to model updating.

3.2.1 Design Sensitivity and Optimization Method

The CORDS approach[25] for test/analysis correlation uses design sensitivity and optimization methods in a two-step procedure. The first step is to

calculate design sensitivity coefficients by using MSC/NASTRAN. The second step uses the CORDS2 program to read the design sensitivity coefficients and apply optimization theory to identify optimum sets of corrections that minimize the error between test and analysis results with minimum changes to the model.

Calculation of Design Sensitivity Coefficients

Design sensitivity coefficients define the relationship between the modal characteristics and design variables. The model's characteristics are modal frequencies and mode shapes, and design variables can be any structural parameters.

A design sensitivity coefficient relates how much a modal parameter will change for a given change of a design variable. This relationship can be expressed as

$$\frac{\partial \Omega_i^2}{\partial r_j} = \lim_{\Delta r_j \to 0} \left(\frac{\Delta \Omega_i^2}{\Delta r_j} \right), \quad \text{and} \quad \frac{\partial \Phi_i}{\partial r_j} = \lim_{\Delta r_j \to 0} \left(\frac{\Delta \Phi_i}{\Delta r_j} \right) \tag{3.21}$$

Linear perturbation methods[39, 40] are used to calculate design sensitivity coefficients.

Knowing the design sensitivity coefficients, the updated values of the modal parameters can be predicted for a given set of design variable changes.

$$\begin{Bmatrix} \Omega_i^2 \\ \Phi_i \end{Bmatrix} = \begin{Bmatrix} \Omega_{a_i}^2 \\ \Phi_{a_i} \end{Bmatrix} + \sum_{j=1}^{n} \frac{\partial}{\partial r_{a_j}} \begin{pmatrix} \Omega_{a_i}^2 \\ \Phi_{a_i} \end{pmatrix} (r_j - r_{a_j}) \tag{3.22}$$

where

Ω_i = *ith* updated modal frequency

Φ_i = *ith* updated mode shape

Ω_{a_i} = *ith* analytical modal frequency

Φ_{a_i} = *ith* analytical mode shape

r_j = *jth* design variable

r_{a_j} = *jth* analytical design variable

Since the design sensitivity coefficients are calculated using linear perturbation theory, they can accurately predict changes to the model's behavior for small changes of the design variables about the current design state.

The design sensitivity coefficients provide significant insight into the factors to adjust to improve test/analysis correlations. Their usefulness can be significantly enhanced by applying optimization theory to determine an "optimum" set of corrections to be applied to the model.

Optimization Theory

An optimum model update is defined as one that minimizes the differences between test and analysis results with minimum changes to the model. This can be expressed as minimizing a performance index as follows:

$$PI = \sum(SV \text{ Errors}) + \sum(DV \text{ Changes}) \tag{3.23}$$

where SV stands for state variable (modal parameter) and DV for design variable.

The definition of optimum model update from Eq.(3.23) can be stated in two ways. The first term of Eq.(3.23) is used to minimize the difference between test and analysis results. The second term of Eq.(3.23) states that it is better to make a small change to accomplish a given reduction in the modal

parameter error. Therefore, in some cases it is important to minimize error in the modal parameter regardless of the amount of design variable change. In other cases, it may be desirable to minimize design variable changes while accepting moderate modal parameter errors.

The relative importance of minimum error or minimum change is defined using overall weighting factors. So Eq.(3.23) can be rewritten as

$$PI = W_{SVO} \times \sum(SV \text{ Errors}) + W_{DVO} \times \sum(DV \text{ Changes}) \tag{3.24}$$

Also, individual weighting factors for each modal parameter and design variable can be defined to allow a detailed control of selected modes or specific design variables. The complete definition of the performance index, including overall and individual weighting factors, is

$$\begin{aligned} PI &= \left(W_{SVO} \times \sum_{i=1}^{m} \left\{ W_{SVI_i} \times \left| \frac{\begin{pmatrix} \Omega \\ \Phi \end{pmatrix}_i - \begin{pmatrix} \Omega_t \\ \Phi_t \end{pmatrix}_i}{\begin{pmatrix} \Omega_t \\ \Phi_t \end{pmatrix}_i} \right| \right\} \right) \\ &+ \left(W_{DVO} \times \sum_{j=1}^{n} \{ W_{DVI_j} \times |r_j - r_{a_j}| \} \right) \end{aligned} \tag{3.25}$$

where

W_{SVO} = overall weighting factor for the modal parameters

W_{SVI_i} = individual weighting factor for the *ith* modal parameter

$\begin{pmatrix} \Omega_t \\ \Phi_t \end{pmatrix}_i$ = test value of the *ith* modal parameter

$\begin{pmatrix} \Omega \\ \Phi \end{pmatrix}_i$ = updated value of the *ith* modal parameter

W_{DVO} = overall weighting factor for the design variables

W_{DVI_i} = individual weighting factor for the *ith* design variables

Further description of the CORDS design sensitivity and optimization method can be found in Refs.[41, 42, 43].

Chapter 4

PAYLOAD SIMULATOR LABORATORY MODEL (Ref.3)

To serve as a test bed for evaluating experimental procedures for updating analytical models of Space Shuttle payloads, a "payload simulator" laboratory model was designed and fabricated. The design and fabrication of this structure, and the results of preliminary model tests are described in Ref.[3]. Figure 4.1. shows the basic configuration of the model, and Fig.4.2. shows the model suspended on bungee cords from the laboratory ceiling. Three electrodynamic shakers are attached for multi-input modal testing. This payload simulator will be used extensively in future studies of model updating.

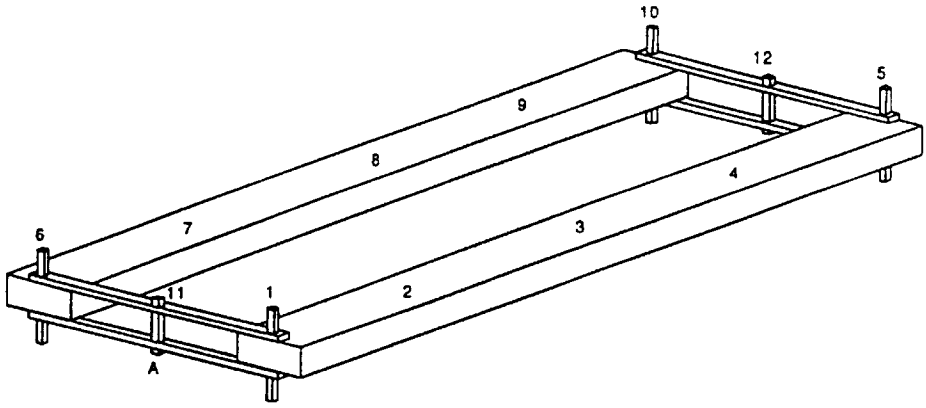

Figure 4.1: Payload simulator configuration.

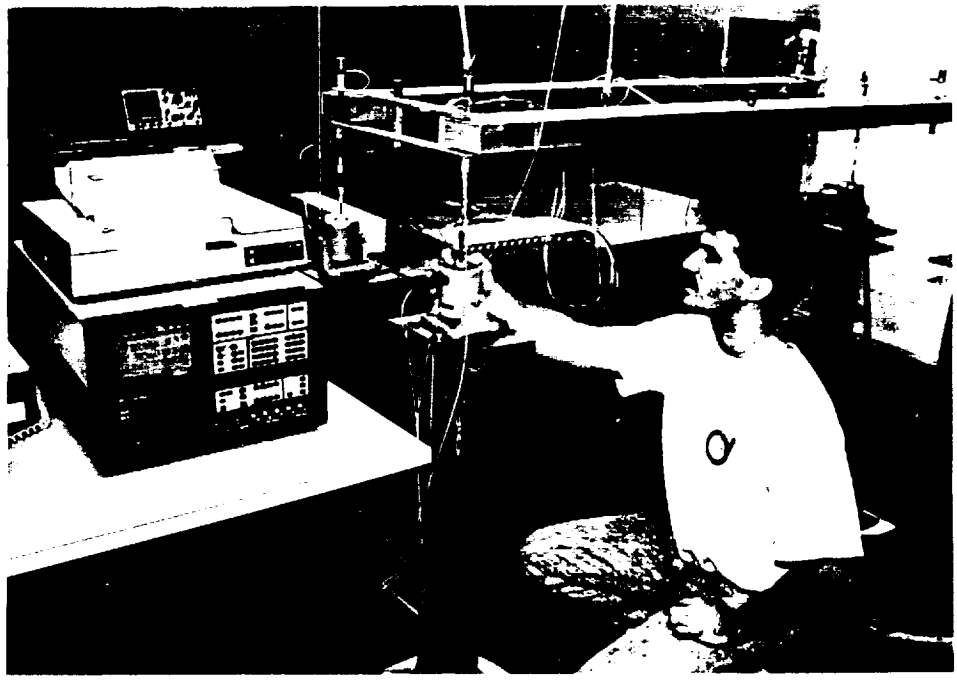

Figure 4.2: Laboratory installation of payload simulator.

Chapter 5

CONCLUSIONS AND RECOMMENDATIONS

This report summarizes three reports that document the research conducted under NASA grant NAG 9-346. Chapter 2 describes methods for using data from free-suspension modal tests to obtain results typically obtained from fixed-base modal tests. Specifically, it is demonstrated that the poles of each element of a frequency response function matrix $[H_{F/U}]$, obtained by testing a system with free boundaries, coincide with the natural frequencies of the same system with fixed boundaries.

Chapter 3 summarizes an extensive literature survey on the topics of error localization and model updating. The methods reviewed are used to incorporate the results of modal testing to improve the fidelity of finite element models.

Finally, Chapter 4 briefly describes a laboratory structure, called a payload simulator, that will be used in further research directed toward the development of model update methods that will be especially applicable to Space Shuttle payloads.

Further research is needed on the following topics:

1. Experiments should be performed, using the payload simulator structure, to assess the feasibility of employing the methods described in Ref.[1] to

obtain fixed-interface modal properties from free-interface modal tests. An error analysis should be performed, and appropriate software should be developed to reduce the free-interface modal test data.

2. Numerical simulations should be performed to compare the various error localization and model updating procedures described in Ref.[2] and the strengths/weaknesses of the various approaches should be assessed.

3. An attempt should be made to develop a model update procedure that takes specific account of the substructure nature of Space Shuttle payloads. The possibility of using this procedure to verify/update analytical models of Space Station substructures that will be delivered to orbit as Space Shuttle payloads should be investigated.

BIBLIOGRAPHY

[1] Li, Chee Yun, and Craig, R. R., Jr.,"System Identification and Model Updating for Structural Components," *Report CAR 90-2*, Center for Aeronautical Research, The University of Texas at Austin, Austin, TX, 78712, April 1990.

[2] Huang, Hsin-Hsen, and Craig, R. R., Jr.,"A Review of Error Localization and Model Updating for Structural Components," *Report CAR 91-1*, Center for Aeromechanics Research, The University of Texas at Austin, Austin, TX, 78712, April 1991.

[3] Barlow, Mark; Harding, Brent; and Wilborn, James, "Space Shuttle Payload Modeling and Testing," *Final Report, ASE363Q*, Department of Aerospace Engineering and Engineering Mechanics, The University of Texas at Austin, Austin, TX, 78712, May 1989.

[4] Coleman, A.D., et. al., "A Mass Additive Technique for Modal Testing as Applied to the Space Shuttle Astro-1 Payload," *Proc. 6th International Modal Analysis Conference*, Kissimee, FL, 1988, pp.154-159.

[5] Brillhart, R.D., et.al., "Transfer Orbit Stage Modal Survey, Part 1, Measurement of Free-Free Modes and Residual Flexibility," *7th International Modal Analysis Conference*, Las Vegas, NV, February 1989.

[6] Brillhart, R.D., et.al.,"Transfer Orbit Stage Modal Survey, Part 2, Measurement of Free-Free Modes and Residual Flexibility," *7th International Modal Analysis Conference*, Las Vegas, NV, February 1989.

[7] Stroeve, A., "Modal Survey Testing of the Combined Release and Radiation Effects Satellite - A Shuttle Payload," *5th International Modal Analysis Conference*, London, England, 1987, pp.1084-1090.

[8] *PAM-DII 37" PAF Modal Survey Test*, Mcdonnell Douglas Astronautics Co. Huntington Beach, CA, 1984.

[9] Blair, M.A., and Vadlamudi, N., "Constrained Structural Dynamic Model Verification Using Free Vehicle Suspension Testing Methods," *29th AIAA/ASME/ASCE/AHS SDM Conference*, Williamsburg, VA, April 1988, Paper No. AIAA-88-2359-CP, pp. 1187-1193.

[10] *Space Shuttle Payload Design and Development, Structural/Mechanical Interfaces and Requirements*, Rev. C., NSTS 20052, Vol.8, NASA-Lyndon B. Johnson Space Center, June 1988.

[11] Craig, R.R., Jr., and Bampton, M. C. C., "Coupling of Substructures for Dynamic Analysis," *AIAA Journal*, Vol. 6, 1968, pp. 1313-1319.

[12] Craig, R.R., Jr., *Structural Dynamics — An Introduction to Computer Methods*, John Wiley & Sons, New York, NY, 1981.

[13] Craig, R.R., Jr., "A Review of Time-Domain and Frequency-Domain Component Mode Synthesis Methods," *The International Journal of Analytical and Experimental Modal Analysis*, Vol. 2, No. 2, April 1987, pp. 59-72.

[14] "Modal Analysis Theory," *Modal Analysis 9.0 Users Manual*, Chapter 6, Structural Dynamics Research Corp. and General Electric CAE International Inc., Milford, OH, 1985.

[15] Becker, E. B., and Craig, R. R., Jr., *ISMIS — Interactive Structures and Matrix Interpretive System: User's Manual with Programmer's Guide*, Department of Aerospace Engineering and Engineering Mechanics, The University of Texas at Austin, Austin, TX, July 1983.

[16] Bangert, S.; Little, J.; and Moler, C. *PC-MATLAB — User's Guide*, The Math Works Inc., Sherborn, MA, 1987.

[17] Sidhu, J. and Ewins, D. J.,"Correlation of Finite Element and Modal Test Studies of a Practical Structure," *2nd International Modal Analysis Conference*, 1984, pp.756-762.

[18] Lieven, N. A. J. and Ewins, D. J., "Error Location and Updating of Finite Element Models Using Singular Value Decomposition," *8th International Modal Analysis Conference*, 1990, pp.768-773.

[19] Fissette, E. and Ibrahim, S., "Error Location and Updating of Analytical Dynamic Models Using a Force Balance Method," *6th International Modal Analysis Conference*, 1988, pp.1063-1070.

[20] Lin, Cheng S., "Location of Modeling Errors Using Modal Test Data," *30th AIAA Structures, Structural Dynamics and Materials Conference*, Paper 89-1240-CP, 1989, pp.713-720. Also, *AIAA Journal*, Vol.28, No.9, Sept. 1990, pp.1650-1654.

[21] Chou, C. M., O'Callahan, J. C. and Wu, C. H., "Localization of Test/Analysis Structural Model Errors," *30th AIAA Structures, Structural Dynamics and Materials Conference*, 1989, pp.748-752.

[22] Ewins, D. J., He, J. and Lieven, N., "A Review of the Error of Matrix Method (EMM) for Structural Dynamic Model Comparison," *Proc. International Conference: Spacecraft Structures and Mechanical Testing*, Noordwijk, The Netherlands, October 1988, pp.55-62.

[23] Ojalvo, I. U. and Pilon, D., "Diagnostics for Geometrically Locating Structural Math Model Errors from Modal Test Data," *29th AIAA Structures, Structural Dynamic and Material Conference*, 1988, pp.1174-1186.

[24] Collins, J. D., Hart, G. C., Hasselman, T. K. and Kennedy, B., "Statistical Identification of Structures," *AIAA Journal*, Vol.12, February 1974, pp.185-190.

[25] CORDS2 User's Manual, Version 1.0, *Structural Dynamics Research Corporation, Engineering Services Division*, San Diego, California, December 31, 1988.

[26] Berman, A. and Flannelly, W. G., "Theory of Incomplete Models of Dynamic Structures," *AIAA Journal*, Vol.9, No.8, August 1971, pp. 481-1487.

[27] Baruch, M. and Bar Itzhack, I. Y., "Optimal Weighted Orthogonalization of Measured Modes," *AIAA Journal*, Vol.16, April 1978, pp.346-351.

[28] Baruch, M., "Methods of Reference Basis for Identification of Linear Dynamic Structures," *AIAA Journal*, April 1982, pp.561-564.

[29] Berman, A. and Nagy, E. J., "Improvement of a Large Analytical Model Using Test Data," *AIAA Journal*, Vol.21, No.8, August 1983, pp.1168-1173.

[30] Chen, S. Y. and Fuh, J. S., "Application of Generalized Inverse in Structural System Identification," *AIAA Journal*, Vol.22, December 1984, pp.1827-1828.

[31] O'Callahan, J. C. and Leung, R., "Optimization of Mass and Stiffness Matrices Using a Generalized Inverse Technique on the Measured Modes," *Proc. 3rd International Modal Analysis Conference* , Orlando, FL., January 1985, pp.75-79.

[32] Chen, J. C. and Garba, J. A. "Analytical Model Improvement Using Modal Test Results," *AIAA Journal*, Vol.18, No.6, June 1980, pp.684-690.

[33] Chen, J. C., Kuo, C. P. and Garba, J. A., "Direct Structural Parameter Identification by Modal Test Results," *Proc. of 24th Structures, Structural Dynamics and Materials Conference*, AIAA paper 83-0812, May 1983, pp.44-49.

[34] Kabe, A. M., "Stiffness Matrix Adjustment Using Mode Data," *AIAA Journal*, Vol.23, No.9, September 1985, pp.1431-1436.

[35] Wei, F. S., "Analytical Dynamic Model Improvement Using Vibration Test Data," *AIAA Journal*, Jan. 1990, pp.175-177.

[36] Wei, F. S. and Zhang D. W., "Mass Matrix Modification Using Element Correction Method," *AIAA Journal*, Jan. 1989, pp.119-121.

[37] Lapierre, Helene and Ostiguy, Germain, "Structural Model Verification With LQO Theory," *29th Structures, Structural Dynamics and Materials Conference*, 1988, pp.1194-1201. Also, *AIAA Journal*, Vol.28, No.8, Aug. 1990, pp.1497-1503.

[38] Janter, T., Heylen, W. and Sas, P., "Practical Application of The UA Model Updating Scheme," *8th International Modal Analysis Conference*, 1990, pp.173-179.

[39] MSC/NASTRAN User Manual, Volume 1, Section 1.14, "Design Sensitivity Analysis," the MacNeal-Schwendler Corporation, Los Angeles, CA., Nov. 1988.

[40] MSC/NASTRAN Application Manual, Volume 2, Section 3.4, "Design Sensitivity Analysis in MSC/NASTRAN," the MacNeal-Schwendler Corporation, Los Angeles, CA., April 1983.

[41] Flanigan, C. C., "Test/Analysis Correlation of the STS Centaur Using Design Sensitivity and Optimization Methods," *5th International Modal Analysis Conference*, 1987, pp.99-107.

[42] Flanigan, C. C., "Test/Analysis Correlation Using Design Sensitivity and Optimization," *Society of Automotive Engineers*, SAE Technical Paper Series 871743, Aerospace Technology Conference and Exposition, Long Beach. A, October 5-8, 1987.

[43] Flanigan, C. C., "Test/Analysis Correlation Using Design Sensitivity and Optimization - Does It Work?," *Society of Automotive Engineers*, SAE

Technical Paper Series 881531, Aerospace Technology Conference and Exposition, Anaheim, CA, October 3-6, 1988.